Small molecules capable of activating DNA methylation–repressed genes targeted by the p38 mitogen-activated protein kinase pathway

Received for publication, November 10, 2017, and in revised form, March 5, 2018 Published, Papers in Press, March 20, 2018, DOI 10.1074/jbc.RA117.000757

Xiang Li[‡§¶], Erchang Shang[‖], Qiang Dong[§¶], Yingfeng Li[§¶], Jing Zhang[¶‖], Shaohua Xu[¶], Zuodong Zhao[§¶], Wei Shao[¶], Cong Lv[‡‡], Yong Zheng[§], Hailin Wang[‡‡], Xiaoguang Lei[‖], Bing Zhu[‡§ §§1], and Zhuqiang Zhang[§2]**

*From the [‡]Graduate School of Peking Union Medical College, Chinese Academy of Medical Sciences, Beijing 100730, China, the [§]National Laboratory of Biomacromolecules, Institute of Biophysics, Chinese Academy of Sciences, Beijing 100101, China, the [¶]National Institute of Biological Sciences, Beijing 102206, China, the [‖]Beijing National Laboratory for Molecular Sciences, Key Laboratory of Bioorganic Chemistry and Molecular Engineering of the Ministry of Education, Department of Chemical Biology, College of Chemistry and Molecular Engineering, Synthetic and Functional Biomolecules Center, and Peking-Tsinghua Center for Life Sciences, Peking University, Beijing 100871, China, the **College of Life Sciences, Beijing Normal University, Beijing 100875, China, the [‡‡]State Key Laboratory of Environmental Chemistry and Ecotoxicology, Research Center for Eco-Environmental Sciences, Chinese Academy of Sciences, Beijing 100085, China, and the [§§]College of Life Sciences, University of Chinese Academy of Sciences, Beijing 100049, China*

Edited by John M. Denu

Regulation of gene expression by epigenetic modifications such as DNA methylation is crucial for developmental and disease processes, including cell differentiation and cancer development. Genes repressed by DNA methylation can be derepressed by various compounds that target DNA methyltransferases, histone deacetylases, and other regulatory factors. However, some additional, unknown mechanisms that promote DNA methylation–mediated gene silencing may exist. Chemical agents that can counteract the effects of epigenetic repression that is not regulated by DNA methyltransferases or histone deacetylases therefore may be of research interest. Here, we report the results of a high-throughput screen using a 308,251-member chemical library to identify potent small molecules that derepress an EGFP reporter gene silenced by DNA methylation. Seven hit compounds were identified that did not directly target bulk DNA methylation or histone acetylation. Analyzing the effect of these compounds on endogenous gene expression, we discovered that three of these compounds (compounds LX-3, LX-4, and LX-5) selectively activate the p38 mitogen-activated protein kinase (MAPK) pathway and derepress a subset of endogenous genes repressed by DNA methylation. Selective agonists of the p38 pathway have been lacking, and our study now provides critical compounds for studying this pathway and p38 MAPK–targeted genes repressed by DNA methylation.

DNA methylation-regulated gene expression plays important roles in development and disease processes, including cell differentiation and cancer development (1–3). In general, methylated DNA in the promoter region restricts transcription and is considered a repressive epigenetic marker (4). Transcriptional dysregulation caused by aberrant DNA methylation can lead to an increasing number of human diseases (3). Cancer cells are often associated with hypomethylation at repeat-rich heterochromatin regions and hypermethylation at the promoter regions of tumor suppressor genes (5–8). In addition, DNA methylation changes in certain loci can directly cause certain neurological diseases, including fragile X syndrome, Friedreich's ataxia, and spinal muscular atrophy, which can be caused by DNA hypermethylation on the promoter regions of the *FMR1* (9), *FXN* (10), and *SMN* genes (11), respectively. Thus, small molecules that can activate genes silenced by DNA methylation are of clinical relevance.

Methylated DNA can be recognized by methyl-CpG–binding domain proteins, which in turn recruit histone deacetylases (HDACs)[3] to ensure gene silencing (12–17). Various inhibitors of DNA methyltransferases (DNMTs) and

This work was primarily supported by China Natural Science Foundation Grant 31571344 (to Z. Z.). This work was also supported by China Natural Science Foundation Grants 31521002, 31425013, 31730047, and 31530037 (to B. Z.); Chinese Ministry of Science and Technology Grants 2015CB856200 and 2016YFA0100400 (to B. Z.); Strategic Priority Research Program Grant XDB08010103 (to B. Z.); and Youth Innovation Promotion Association Grant 2017133 (to Z. Z.) of the Chinese Academy of Sciences. The authors declare that they have no conflicts of interest with the contents of this article.

This article contains Figs. S1–S8.

The high throughput sequencing data have been deposited to the GEO database and are available under accession ID GSE106573.

[1] To whom correspondence may be addressed. Tel.: 86-10-64888832; Fax: 86-10-64888832; E-mail: zhubing@ibp.ac.cn.

[2] To whom correspondence may be addressed. Tel.: 86-10-64888213; E-mail: zhangzhuqiang@ibp.ac.cn.

[3] The abbreviations used are: HDAC, histone deacetylase; MeDIP-seq, methylated DNA immunoprecipitation followed by sequencing; DNMT, DNA methyltransferase; 5-aza-dC, 5-aza-2′-deoxycytidine; TF, transcription factor; EGFP, enhanced green fluorescent protein; CMV, cytomegalovirus; TSA, trichostatin A; GO, gene ontology; MAPK, mitogen-activated protein kinase; TNF, tumor necrosis factor; ERK, extracellular signal-regulated kinase; JNK, c-Jun N-terminal kinase; SAPK, stress-activated protein kinase; GSEA, gene set enrichment analysis; TSS, transcription start site; EGF, epidermal growth factor; CRE, cAMP-binding element; CREB, CRE-binding protein; PI3K, phosphatidylinositol 3-kinase; bp, base pair(s); FBS, fetal bovine serum; qPCR, quantitative PCR; UHPLC, ultra-high-performance liquid chromatography; MRM, multiple-reaction monitoring; 5mC, 5-methylcytosine; 5hmC, 5-hydroxymethylcytosine; RPKM, reads per kilobase per million total reads.

HDACs have been identified, and many of them can derepress various sets of genes repressed by DNA methylation (18–23). Some of these compounds, including inhibitors of DNMTs, such as 5-aza-cytidine and 5-aza-2′-deoxycytidine (5-aza-dC), and inhibitors of HDACs, such as SAHA, romidepsin, panobinostat, mocetinostat, belinostat, and chidamide, have been approved as anticancer drugs.

However, histone deacetylation is not the sole mechanism for DNA methylation–mediated gene silencing (19, 24, 25, 27, 28). Methylated CpG sites that reside in transcription factor (TF) binding sites can directly block the association of certain TFs and prevent TF-dependent activation (12, 29–31). In addition, unknown mechanisms facilitating DNA methylation–mediated gene silencing may exist. Therefore, identification of novel compounds that can derepress certain genes repressed by DNA methylation, without directly inhibiting DNMTs and HDACs, are of research interest.

Herein, we developed a cell-based screening system and screened against a chemical library containing ~300,000 small molecules. We identified several classes of small molecules that could derepress various sets of genes repressed by DNA methylation. One group of these small molecules targets the p38 MAPK pathway and can activate endogenous MAPK target genes repressed by DNA methylation without directly inhibiting DNMTs and HDACs.

Results

A cell-based imaging assay that monitors activation of a DNA methylation–silenced gene reporter

To identify novel small molecules targeting gene repression, we devised a cell-based high-throughput screening system. To generate the reporter cell line, we first constructed a plasmid containing an enhanced green fluorescence protein (EGFP) reporter that was driven by a CMV promoter. We then methylated it *in vitro* with SssI methyltransferase and co-transfected it into HEK293 cells, together with a construct containing a hygromycin B-resistant gene (Fig. S1). After hygromycin B selection, a stable cell line, termed B2-17, was chosen for screening. B2-17 cells displayed a low background EGFP signal (Fig. 1*A*) and were highly methylated at the CMV promoter (Fig. 1*B*). Treatment with 5 μM 5-aza-dC resulted in robust EGFP reactivation, and treatment with 100 nM trichostatin A (TSA), a potent HDAC inhibitor, also reactivated the reporter gene, albeit to a lesser extent than 5-aza-dC treatment (Fig. 1*A*).

A high-throughput chemical screen

Using the B2-17 cell line, we performed an image-based compound screening using a chemical library containing 308,251 small molecules (Fig. 1*C*). This library had no specific focus and was a collection purposed for unbiased compound screening, which had been used in a variety of studies (32–35).

The cells were treated with 10 μM aliquots of each compound for 72 h before imaging, and the mean percentage of EGFP$^+$ cells (R_{GFP}) was calculated for each compound. In summary, 1,597 compounds (0.5%) reactivated the EGFP reporter in at least 15% of cells, and 363 compounds (0.12%) reactivated the EGFP reporter in >50% of cells (Fig. 2*A*).

We chose these 363 compounds as the primary hits and then evaluated them with two additional reporter cell lines, C3-2 (with a methylated CMV-EGFP) and 5C46-11 (with a methylated CMV-RFP), which were established using similar protocols (Figs. S1 and S2). One hundred eighty-five compounds reactivated reporter genes in >50% of cells in all three cell lines, and these were selected as the secondary hits.

Next, we performed titration experiments for all of the secondary hits in the B2-17 cell line. The efficacy of each compound was evaluated by its maximal R_{GFP} value (Fig. 2*B*) and relative half-maximal effect concentration (EC_{50}) (Fig. 2*C*). In parallel, we also analyzed the toxicity of each secondary hit by measuring the number of viable cells in each treatment, based on quantitation of ATP, an indicator of metabolically active cells. For each compound, we calculated the relative half-maximal growth-inhibitory concentration (IC_{50}), based on the above-mentioned assay (Fig. 2*C*).

After these measurements, we decided to focus on seven hit compounds that met the following three criteria: maximal $R_{GFP} >$ 60% (good response rate) (Fig. 2*B* and Fig. S3*A*), $EC_{50} < 5$ μM (good efficacy) (Fig. 2*C* and Fig. S3*B*), and $IC_{50} > 3$ μM (less toxic) (Fig. 2*C* and Fig. S3*C*). We termed these seven compounds LX-1 to LX-7 for simplicity (Fig. 2*D*). Notably, the molecular formulae of the seven hit compounds were distinct from each other and did not resemble known compounds that target epigenetic regulators.

No alteration of global DNA methylation or histone acetylation upon treatment with hit compounds

To understand whether these hit compounds directly target DNA methyltransferase or histone deacetylases, we examined the levels of DNA methylation and bulk histone acetylation. UHPLC-MRM MS/MS results showed that no significant changes in bulk 5mC level were observed in C3-2 cells treated with any of these compounds (72-h treatment), whereas 5-aza-dC treatment clearly reduced the bulk 5mC level (Fig. 3*A*).

We also tested whether these hit compounds caused site-specific DNA demethylation at the reporter gene. Bisulfite sequencing results of the CMV promoter of the integrated reporter gene revealed that the changes in DNA methylation level after treatment with TSA or the hit compounds were relatively modest, whereas the effect of 5-aza-dC treatment was apparent (Fig. 3*B*). These results suggested that none of the hit compounds directly targeted the DNA methylation machinery.

We then examined the bulk histone acetylation level of cells treated with these hit compounds. The positive controls, sodium butyrate and TSA, caused a robust global increase in histone H4 acetylation. However, none of the seven hit compounds was able to do so (Fig. 3*C*). These results suggested that none of the hit compounds were pan-histone deacetylase inhibitors.

Hit compounds activate endogenous genes

We next tested whether these hit compounds could activate endogenous genes. First, to focus on genes silenced by DNA methylation, we performed MeDIP-seq (methylated DNA

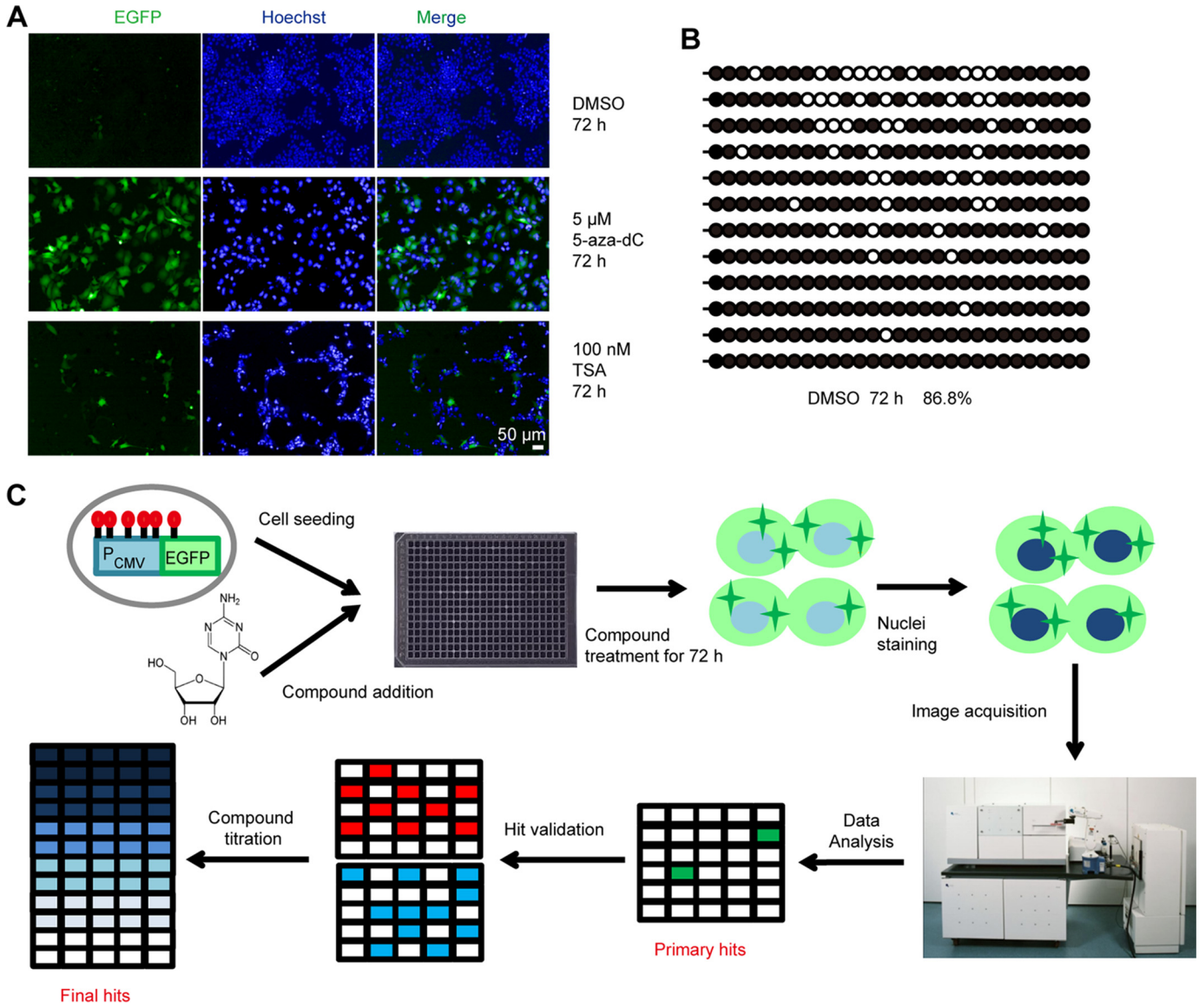

Figure 1. High-content chemical screen for potential epigenetic modulators. *A*, confocal images of B2-17 cells after treatment with 5-aza-dC and TSA. 5-aza-dC and TSA can stimulate 89 and 11% of cells to express EGFP at the indicated concentration. DMSO (0.5%) vehicle (no treatment) was used as a negative control. EGFP (*green*) and Hoechst 33342 nucleus staining (*blue*) are shown. *B*, methylation level of CMV promoter of reporter gene in B2-17 cells. *Black* and *white circles* indicate methylated and unmethylated CpG sites, respectively. The percentage of methylated CpG sites is indicated *below*. *C*, scheme of the chemical screen. The map of the EGFP reporter is shown. B2-17 cells were treated with the compound library in 384-well plates. Cell nuclei were stained with Hoechst 33342. In each 384-well plate, 0.5% DMSO vehicle (no treatment) and the positive controls 5-aza-dC and TSA were added.

immunoprecipitation followed by sequencing) experiments in B2-17 cells and selected a list of genes with a high level of DNA methylation at promoters or CpG islands, including *TNF*, *EGR1*, *LY6K*, and *ISG20* (Fig. S4). Among these, *TNF* (36, 37) and *LY6K* (38) were reported to be silenced by DNA methylation in various cell types. These genes could be activated by 5-aza-dC treatment (Fig. 4*A*). Treatment with compounds LX-1, LX-3, LX-4, and LX-5 effectively activated the expression of all of the above selected genes. Compounds LX-2 and LX-6 activated a portion of these genes with less efficiency, and compound LX-7 selectively activated the expression of *TNF* and *ISG20* (Fig. 4*A*). These results suggested that some of the above compounds probably have different targets.

To further study the roles of these hit compounds in regulating gene expression, we performed RNA-seq experiments using B2-17 cells treated with these seven compounds, 5-aza-dC, or RG108, another inhibitor of DNA methyltransferase (39). Genes up- or down-regulated >2-fold upon compound treatment, compared with DMSO-treated control samples, were defined as up- or down-regulated genes for each compound treatment. Several compounds displayed a clear effect on gene activation because treatments with these compounds resulted in far more up-regulated genes than down-regulated genes. These compounds include LX-1 (981 up *versus* 406 down), LX-3 (1,223 up *versus* 364 down), LX-4 (1,064 up *versus* 422 down), LX-5 (1,492 up *versus* 460 down), and LX-6 (209 up *versus* 39 down) (Fig. 4*B*). A similar biased effect was much less apparent for compounds LX-2 and LX-7 (Fig. 4*B*), suggesting that these two compounds were unlikely to play direct roles in gene activation.

A

Library	Compound number	Hit compound number		
		R_{GFP} > 50%	30% < R_{GFP} < 50%	15% < R_{GFP} < 30%
Maybridge	14,402	15	16	32
Enamine	22,001	9	47	56
Specs	30,335	48	82	105
Chemdiv	100,413	165	173	335
WXTD	141,100	126	134	254
Sum	308 ,251	363 (0.12%)	452 (0.15%)	782 (0.25%)

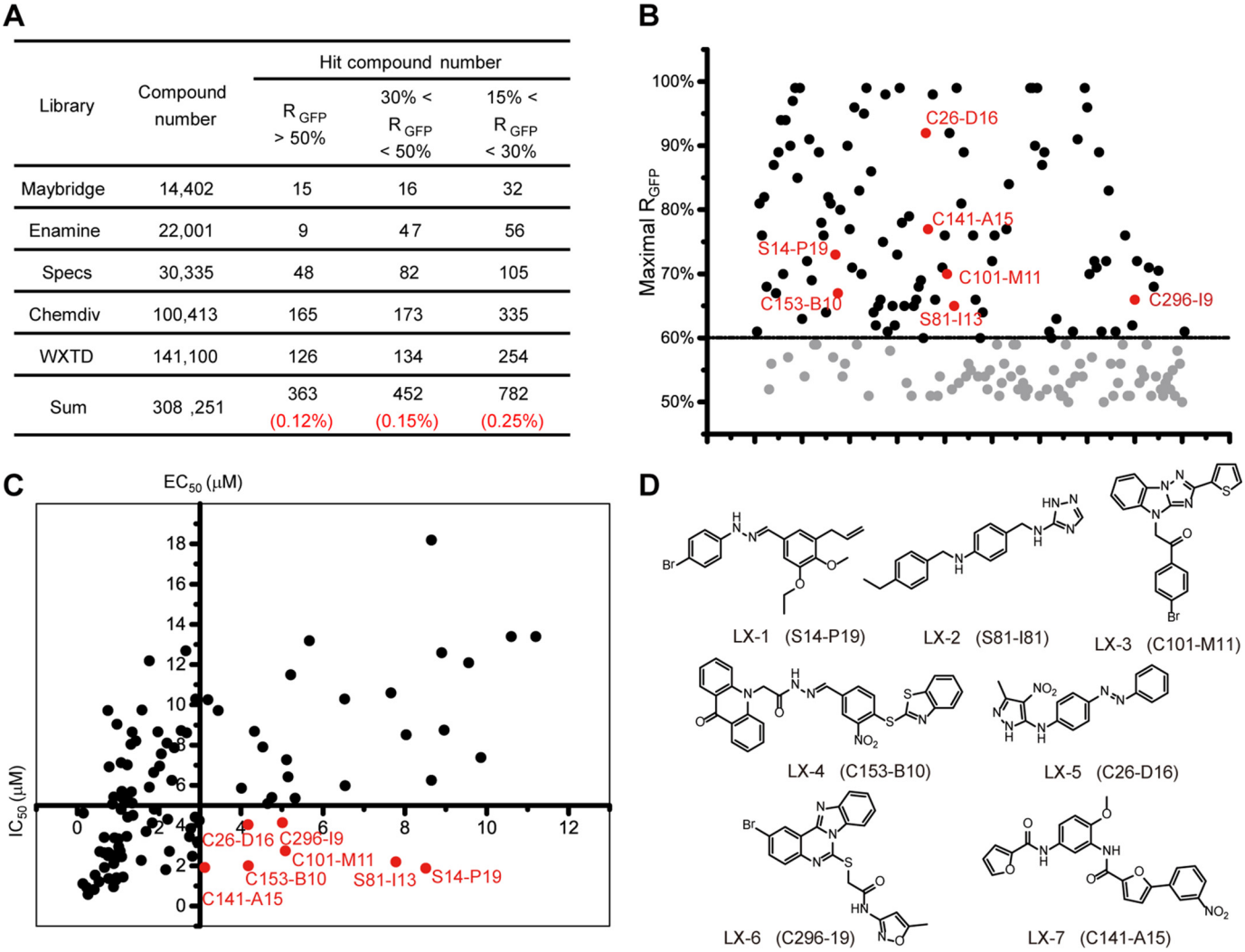

Figure 2. Three rounds of selection identified the seven best hits. *A*, statistics results of primary hits. This screen was against five libraries. A cut-off threshold was set at 15%. Primary hits were classified into three groups by the percentage of reactivated cells under each treatment. *Red numbers* indicate the percentage of each group in the whole library. *B*, validation of candidate hits by the maximal percentage of $EGFP^+$ cells (maximal R_{GFP}) of each secondary hit. Distributions of the maximal R_{GFP} values of 185 hits are shown. The maximal R_{GFP} value is the mean percentage of $EGFP^+$ cells (R_{GFP}) in the platform concentration. The cut-off threshold of maximal effect was 60% (*dotted line*). *C*, validation of candidate hits by half-maximal growth-inhibitory concentration (IC_{50}) and half-maximal effect concentration (EC_{50}) of each secondary hit. Distributions of IC_{50}-EC_{50} of 185 hits are shown. The cut-off thresholds for IC_{50} and EC_{50} were 3 and 5 μM, respectively. *Red dots* indicate the eight best hits. *D*, structures of the seven best hits.

We then performed unsupervised clustering analysis and noticed that hit compounds LX-3, LX-4, and LX-5 appeared to be closely related (Fig. 4*C*). Indeed, the majority of genes up-regulated by compounds LX-3, LX-4, and LX-5 overlapped with each other (Fig. 4*D*), although these three compounds have distinct molecular structures (Fig. 2*D*). These results suggested that these three compounds may function in the same pathway, and we decided to focus our study on them.

Compounds LX-3, LX-4, and LX-5 are connected with the MAPK pathway

To understand what kind of biological processes and pathways were targeted by compounds LX-3, LX-4, and LX-5, we performed gene ontology (GO) enrichment analysis for the 795 genes that were commonly up-regulated by treatments with compounds LX-3, LX-4, and LX-5. The clustering map of GO terms and the corresponding gene sets showed two major categories. One of these was related to secreted proteins and membrane proteins, and the other was related to the viral infection response (Fig. 5*A*). Consistently, KEGG pathway enrichment analysis also revealed the enrichment of several signaling pathways and immune-related processes, including the MAPK pathway and the closely related TNF pathway (Fig. 5*B*).

In general, MAPKs are categorized into four subgroups: 1) extracellular signal-regulated kinases (ERKs), 2) c-Jun N-terminal or stress-activated protein kinases (JNK/SAPK), 3) ERK5/big MAPK 1 (BMK1), and 4) the p38 group of protein kinases (40). Among these, ERKs, JNK/SAPK, and p38 kinase constitute the main network (Fig. S5). To further examine the relationship between the MAPK pathway and treatment with compounds LX-3, LX-4, and LX-5, we performed gene set enrichment analysis (GSEA) to compare the >795 genes that were commonly up-regulated by treatment with compounds LX-3, LX-4, and LX-5 with published gene sets that were regulated by TNF signaling (41) (MSigDB set M2496), the ERK1/2 cascade (genes annotated under GO:0070372, MSigDB set M12990), and JNK

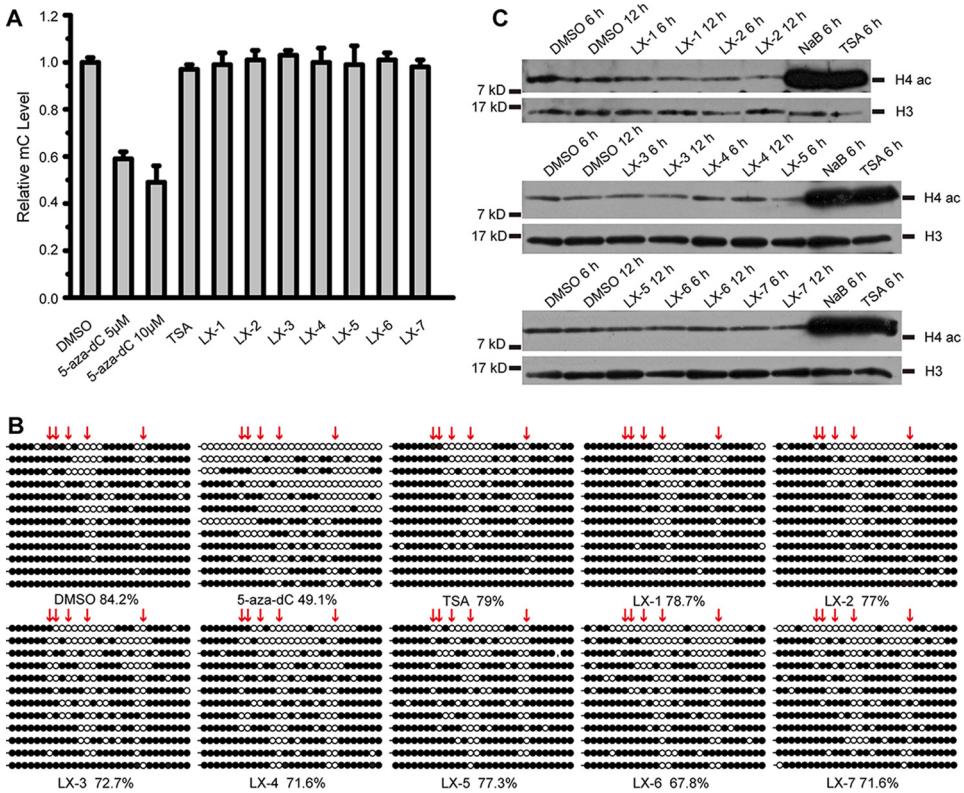

Figure 3. Effect of seven compounds on DNA methylation and histone acetylation. *A*, UHPLC-MRM MS/MS quantitation of 5mC levels of genomic DNA from cells treated with compounds LX-1 to LX-7, 5-aza-dC, and TSA. *Error bars*, S.D. of three biological replicates. *B*, bisulfite sequencing results of the CMV promoter of the reporter gene in cells treated with compounds LX-1 to LX-7, 5-aza-dC, and TSA. *Black* and *white circles* represent methylated and unmethylated CpG sites, respectively. The percentages of methylated CpG sites are indicated. *C*, representative Western blot showing the effects of compounds LX-1 to LX-7 on histone acetylation level. Histone acetylation levels were examined after 6 or 12 h of treatment. Two HDAC inhibitors, sodium butyrate (NaB) and TSA, were used as positive controls. Histone H3 was used as a loading control.

knockdown (42) (MSigDB set M2745). The gene set responsive to TNF signaling was significantly enriched, and the gene set responsive to the ERK1/2 cascade was also enriched (Fig. 5*C*). These data also suggest that compounds LX-3, LX-4, and LX-5 may affect the MAPK pathway.

MAPK pathway activation regulates gene expression through its downstream transcription factors, and many of these are also up-regulated upon MAPK pathway activation (43–45). We focused on transcription factors that were up-regulated upon treatment, and we identified 21 such transcription factors whose binding sites were enriched around the transcription start sites (TSSs) (TSS ± 2 kb) of the 795 genes commonly up-regulated by compounds LX-3, LX-4, and LX-5 (Fig. 5*D*). Notably, these factors included several oncogenic factors, including JUN, JUND, FOS, and FOSB. We next analyzed these 21 transcription factors with the STRING database, which contains known and predicted protein-protein interactions, including physical and functional associations (46). STRING analysis of these 21 transcription factors identified a functionally linked network with high confidence (>0.7), which contained several proteins related to the MAPK pathway (FOS, FOSB, FOSL1, FOSL2, JUNB, JUN, JUND, BCL3, and EGR1) and centered on JUN, JUNB, and FOS (Fig. 5*E*). This network probably serves as a core regulatory module for the gene activation role of compounds LX-3, LX-4, and LX-5. Taken together, the above analyses suggest that the activation effects of compounds LX-3, LX-4, and LX-5 are probably via the activation of the MAPK pathway and its downstream transcription factors.

Compounds LX-3, LX-4, and LX-5 induce phosphorylation of p38 and activation of the p38 pathway

To further study the mechanism of gene activation mediated by treatment with compounds LX-3, LX-4, and LX-5, we examined whether activation of ERKs, JNK/SAPK, and p38 occurred upon treatment with these compounds. In human HEK293 cells, human acute myeloid leukemia cell line MOLM13, and mouse NIH 3T3 cells, treatments with compounds LX-3, LX-4, and LX-5 induced phosphorylation of p38, but these treatments did not cause apparent increases in phosphorylation of ERKs or JNKs (Fig. 6*A* and Fig. S6). In control experiments, anisomycin treatment induced activation of both p38 and JNKs, and EGF treatment induced robust activation of ERKs (Fig. 6*A* and Fig. S6), as reported previously (47–51). From these results, we conclude that compounds LX-3, LX-4, and LX-5 probably function by selectively activating the p38 pathway.

Next, we carried out experiments to determine whether the derepression of the methylated EGFP reporter gene (Fig. 2) and the activation of p38 (Fig. 6*A* and Fig. S6) by treatment with compounds LX-3, LX-4, and LX-5 are separate events or connected events. We chose several inhibitors of the MAPK pathway (FR180204 for ERKs, SB203580 for p38, and SP600125 for JNKs) (52–54) (Fig. S5) and tested whether they could interfere with the activation of the methylated EGFP reporter gene

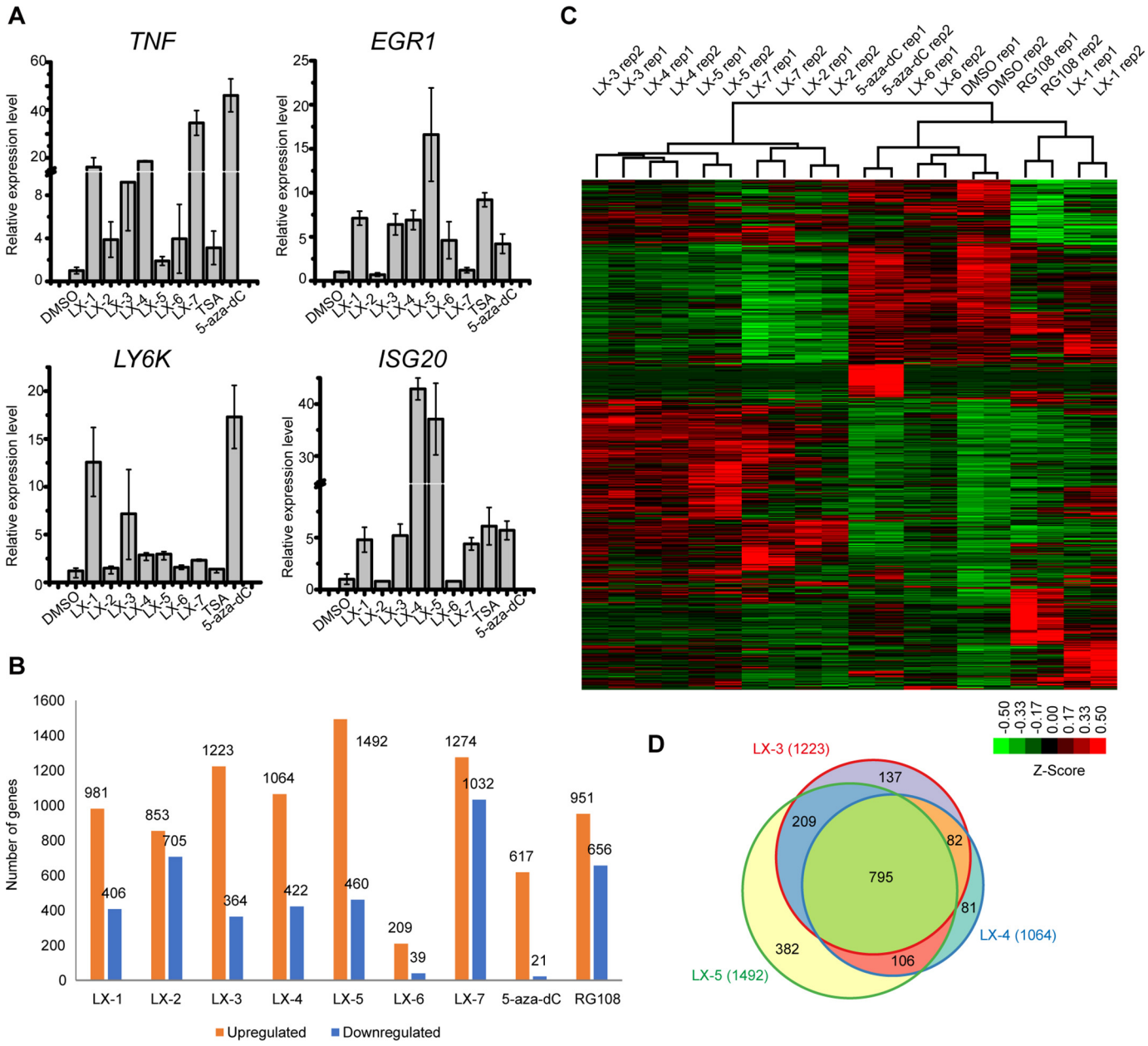

Figure 4. Hit compounds activated a fraction of endogenous genes silenced by DNA methylation. *A*, expression levels of several endogenous genes after treatment with hit compounds. All of these genes are reported to be silenced by DNA methylation. See also Fig. S4*A*. The DNA methylation inhibitor 5-aza-dC and HDAC inhibitor TSA were included as controls. *Error bars*, S.D. from triplicate wells. Data are normalized to the DMSO vehicle control. *B*, histogram showing the up- and down-regulated gene numbers in hit compound–treated cells. The number of genes affected by a given treatment is shown on the *y* axis. *C*, heat map showing the gene expression profile of cells treated with hit compounds. Three DNA methylation inhibitors, 5-aza-dC, procaine, and RG108, were used as controls. *D*, Venn diagrams demonstrating the number of commonly and differentially up-regulated genes in cells treated with compounds LX-3, LX-4, and LX-5.

by treatments with compounds LX-3, LX-4, and LX-5. Only SB203580, a well-known p38 inhibitor (53), reduced the percentage of EGFP$^+$ cells that were activated by treatments with compounds LX-3, LX-4, and LX-5 (Fig. 6*B*).

On the other hand, overexpression of constitutively active forms of two kinases upstream of p38 for 72 h, MKK3 (CA-MKK3, S189E/T193E) and MKK6 (CA-MKK6, S207E/T211E) (55), in B2-17 cells resulted in robust activation of the methylated EGFP reporter gene, but the inactive forms of MKK3 (IA-MKK3, S189A/T193A) and MKK6 (IA-MKK6, K82A) (55) failed to do so (Fig. 7). Taken together, these data show that compounds LX-3, LX-4, and LX-5 exert their function by activating the p38 MAPK pathway, which is capable of activating the methylated EGFP reporter gene.

Compounds LX-3, LX-4, and LX-5 derepress a subset of endogenous methylated genes

Treatment with compounds LX-3, LX-4, and LX-5 derepressed the methylated EGFP reporter gene by activating the p38 MAPK pathway (Fig. 6 and Fig. S6). We then asked whether such an event occurred at endogenous methylated genes. Among the 617 genes activated by 5-aza-dC treatment, 148

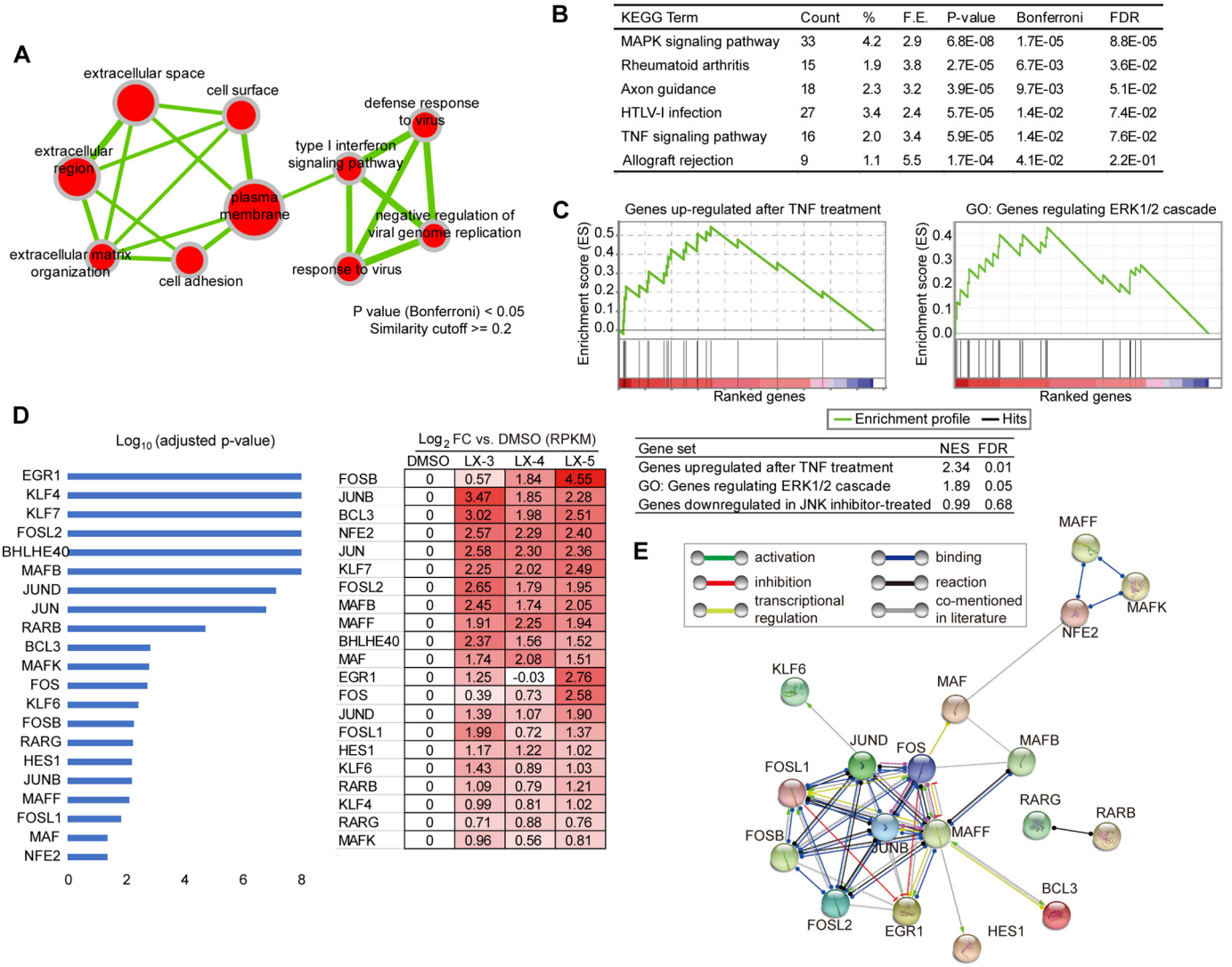

KEGG Term	Count	%	F.E.	P-value	Bonferroni	FDR
MAPK signaling pathway	33	4.2	2.9	6.8E-08	1.7E-05	8.8E-05
Rheumatoid arthritis	15	1.9	3.8	2.7E-05	6.7E-03	3.6E-02
Axon guidance	18	2.3	3.2	3.9E-05	9.7E-03	5.1E-02
HTLV-I infection	27	3.4	2.4	5.7E-05	1.4E-02	7.4E-02
TNF signaling pathway	16	2.0	3.4	5.9E-05	1.4E-02	7.6E-02
Allograft rejection	9	1.1	5.5	1.7E-04	4.1E-02	2.2E-01

Gene set	NES	FDR
Genes upregulated after TNF treatment	2.34	0.01
GO: Genes regulating ERK1/2 cascade	1.89	0.05
Genes downregulated in JNK inhibitor-treated	0.99	0.68

	DMSO	LX-3	LX-4	LX-5
FOSB	0	0.57	1.84	4.55
JUNB	0	3.47	1.85	2.28
BCL3	0	3.02	1.98	2.51
NFE2	0	2.57	2.29	2.40
JUN	0	2.58	2.30	2.36
KLF7	0	2.25	2.02	2.49
FOSL2	0	2.65	1.79	1.95
MAFB	0	2.45	1.74	2.05
MAFF	0	1.91	2.25	1.94
BHLHE40	0	2.37	1.56	1.52
MAF	0	1.74	2.08	1.51
EGR1	0	1.25	-0.03	2.76
FOS	0	0.39	0.73	2.58
JUND	0	1.39	1.07	1.90
FOSL1	0	1.99	0.72	1.37
HES1	0	1.17	1.22	1.02
KLF6	0	1.43	0.89	1.03
RARB	0	1.09	0.79	1.21
KLF4	0	0.99	0.81	1.02
RARG	0	0.71	0.88	0.76
MAFK	0	0.96	0.56	0.81

Figure 5. The functions of compounds LX-3, LX-4, and LX-5 are associated with the MAPK pathway. *A*, GO enrichment analysis of the 795 genes commonly up-regulated by compounds LX-3, LX-4, and LX-5. Enriched terms with FDR *p* value <0.05 are shown. *Circle size* indicates gene set number, and *thickness* of *edges* indicates gene set overlaps. *B*, KEGG pathway enrichment analysis of the 795 genes commonly up-regulated by compounds LX-3, LX-4, and LX-5. *C*, GSEA of the 795 genes commonly up-regulated by treatments with compounds LX-3, LX-4, and LX-5 with three MAPK-related gene sets. *D*, enriched transcription factor binding sites at the promoters of 795 genes commonly up-regulated by compounds LX-3, LX-4, and LX-5 (*left*). Only TFBSs whose corresponding transcription factor was activated by LX-3, LX-4, and LX-5 are shown. Enrichment *p* values (adjusted) were calculated by AME tools from the MEME suite (26). *E*, interaction network of the enriched transcription factors in *D* with high confidence (>0.7) analyzed by STRING database. Genes are represented as nodes, and the biological relationship between two nodes is represented as an edge (*line*).

(24%) overlapped with the 795 genes commonly activated by treatments with compounds LX-3, LX-4, and LX-5, which was 6-fold higher than expected from random overlap (Fig. 8*A*). Among these, several known p38 MAPK target genes (*IL11*, *TNFAIP3*, and *CXCL1*) (41, 56) were included. The promoters or CpG islands of these genes were methylated in HEK293 cells (Fig. 8*B*), and their expression was elevated by 5-aza-dC treatment (Fig. 8*C*) and treatments with compounds LX-3, LX-4, and LX-5 (Fig. 8*D*). Moreover, expression of these three endogenous genes was also up-regulated in human MOLM13 and mouse NIH 3T3 cells treated with 5-aza-dC (Fig. S7, *A* and *B*) and compounds LX-3, LX-4, and LX-5 (Fig. S7, *C* and *D*).

Discussion

Small-molecule screens are most commonly conducted using biochemical assays monitoring the catalytic activities of known enzymes or interaction features of known proteins. In this study, we took an alternative approach and used a cell-based assay to identify small molecules that were capable of activating a DNA methylation–repressed reporter gene. Because of the nature of this approach, two classes of small molecules were likely to be expected in the list of hits. One class of potential hits may directly impact DNA methylation machinery or factors downstream of DNA methylation that are essential for gene silencing, and another class of potential hits may display promoter-specific features and selectively activate a set of genes under the control of a similar pathway. In addition, hit compounds belonging to the latter class should function in a DNA methylation–insensitive manner.

Among the seven hit compounds that we identified, we suspect that five of them (compounds LX-1, LX-3, LX-4, LX-5, and LX-6) may play direct roles in gene activation, because treat-

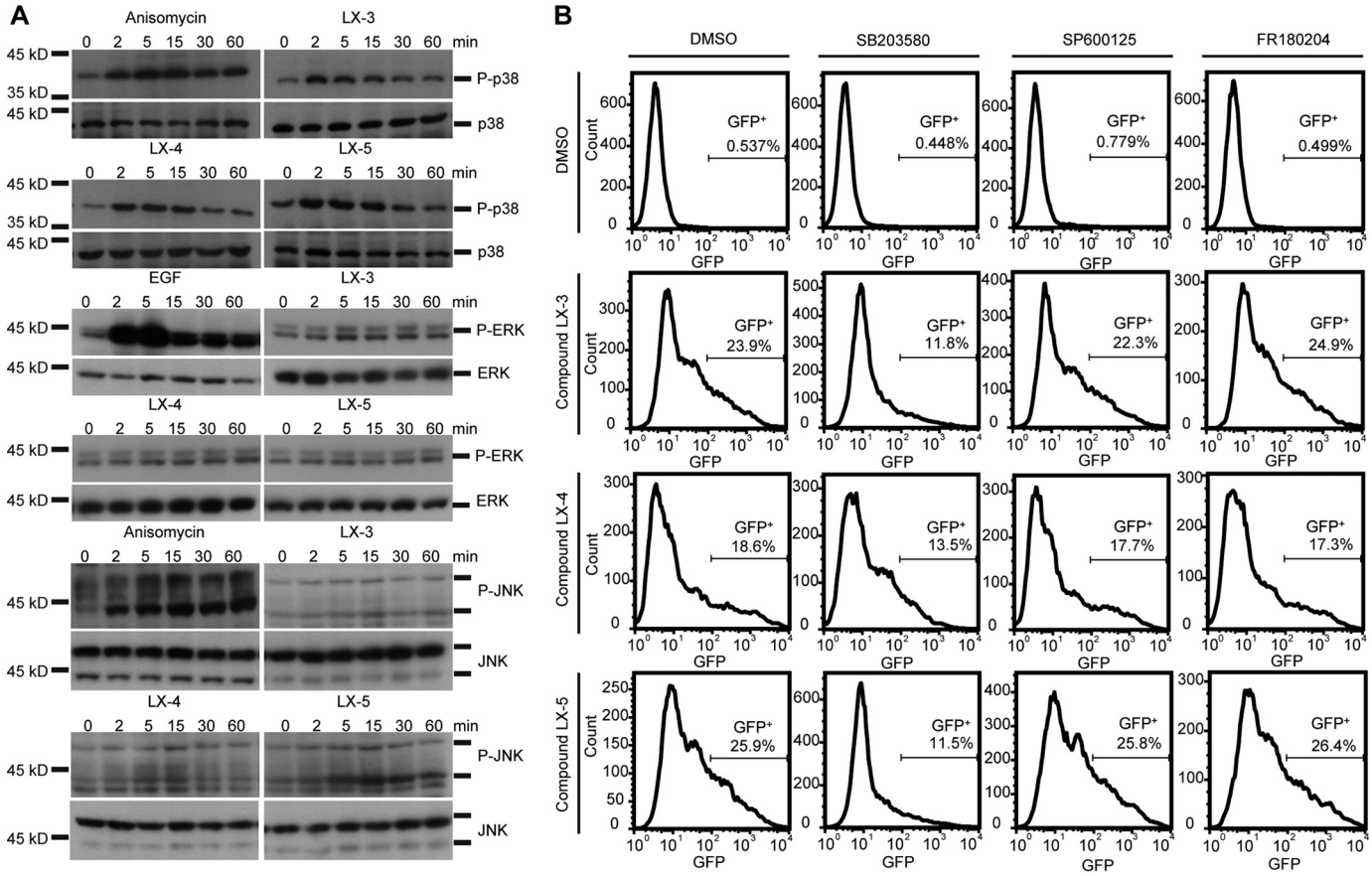

Figure 6. Compounds LX-3, LX-4, and LX-5 function as activators of the MAPK pathway. *A*, representative Western blotting showing the changes in protein levels of JNK, P-JNK, ERK, P-ERK, p38, and P-p38 in HEK293 F cells after treatment with compounds LX-3, LX-4, and LX-5. Anisomycin and EGF were used as positive controls. *B*, effects of inhibitors of the p38 pathway (SB203580), ERK pathway (FR180204), and JNK pathway (SP600125) in preventing the reactivation of the reporter gene by compounds LX-3, LX-4, and LX-5. See also Fig. S5. The percentages of GFP-positive cells indicated on the *right* are displayed.

ment with these compounds resulted in far more up-regulated genes than down-regulated genes (Fig. 4*B*). All of these seven hit compounds have not been reported in any previous screen in the literature, which suggested that they may have new modes of action.

For compounds LX-1 and LX-6, we currently do not fully understand whether they belong to the first class or the second class. Nevertheless, we noticed that compound LX-1 treatment was clustered together with RG108 treatment in a transcriptome analysis (Fig. 4*C*). This suggests that compound LX-1 may directly impact DNA methylation–mediated repression, although treatment with compound LX-1 did not cause global demethylation (Fig. 3*A*). These results hint that compound LX-1 may target events downstream of DNA methylation. However, substantial future investigation is required to clarify this, especially because treatment with compound LX-1 or RG108 did not cluster together with treatment with 5-aza-dC in our transcriptome analysis (Fig. 4*C*). Although RG108 and 5-aza-dC are both inhibitors of DNMTs, their modes of action are different, and they often display different effects on gene regulation (39, 57, 58).

Compounds LX-3, LX-4, and LX-5 probably belong to the second group, because they selectively activate the MAPK pathway (Figs. 5–8). These compounds came into our hit list probably because we used the CMV promoter to drive the EGFP reporter gene, and the CMV promoter is known to be a target of the MAPK pathway (59). The CMV promoter contains binding sites for multiple transcription factors, including NF-κB/RELA, CREB/ATF, AP1, ETS, ELK1, and SP-1 (Fig. S8). Some of these transcription factors, such as the CREB/ATF family of proteins, are known to be sensitive to DNA methylation (60, 61). The CREB/ATF protein family is a group of transcription factors that are activated in response to second messenger cAMP and mitogen or stress signals transduced by MAPK and PI3K-ATK pathways (62–64). A typical cAMP-responsive element (CRE) is an 8-bp palindromic sequence motif (TGACGTCA) (65–67), and the CMV promoter used in this study contained four of these CREs (Fig. S8). Each CRE contains a CpG site, and intriguingly, CREB binding is sensitive to CpG methylation within CRE (60, 61) *in vitro*, yet MAPK activation effectively overcame DNA methylation–mediated repression *in vivo* in our system. A number of potential explanations exist. 1) There are multiple CREB family proteins, and perhaps not all of them are sensitive to CpG methylation during CRE recognition. 2) The CMV promoter contains binding sites for multiple transcription factors, and the association of methylation-insensitive transcription factors such as NF-κB/RELA may facilitate transcriptional activation, which may lead to eventual demethylation of neighboring CpGs within CREs. Consistent with this possibility, we

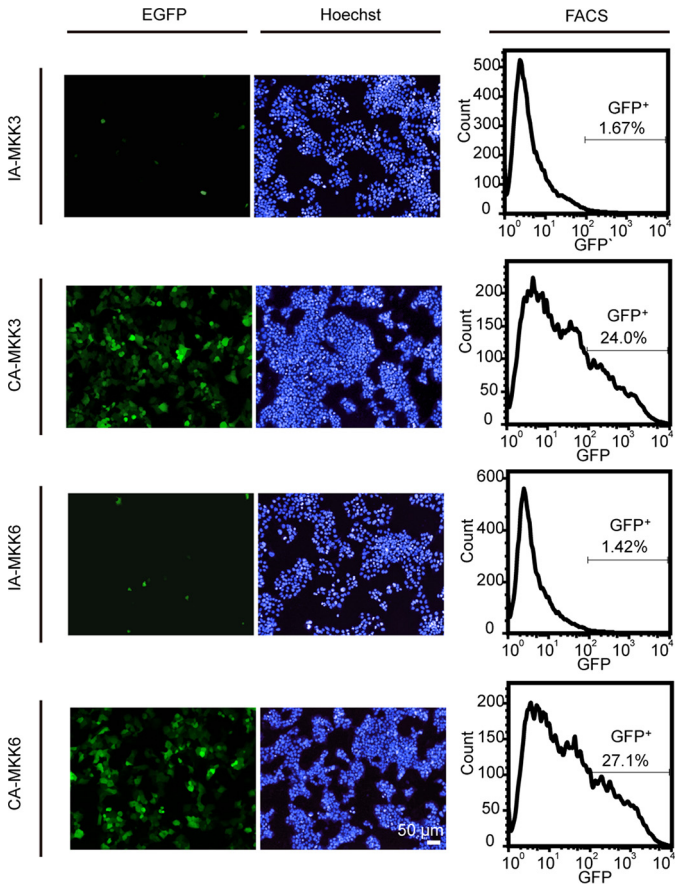

Figure 7. Forced activation of the p38 MAPK pathway by overexpression of CA-MKK3 and CA-MKK6 induces EGFP expression in B2-17 cells. CA-MKK3 and CA-MKK6 are the constitutively active forms of MKK3 and MKK6. IA-MKK3 and IA-MKK6 are the inactive forms of MKK3 and MKK6. EGFP (*green*), Hoechst 33342 nucleus staining (*blue*), and FACS results are shown. The percentages of GFP-positive cells indicated on the *right* are displayed. The FACS results were consistent with the imaging data.

observed reduced CpG methylation at some of the CREs within the CMV promoter (Fig. 3*B*, *red arrows*).

In mammals, the p38 MAPKs could be activated by a number of extracellular stimuli, of which most commonly used include anisomycin, UV light, lipopolysaccharide, TNFα, and some other cytokines and growth factors (40, 68, 69). The reported p38-activating compounds mainly include anisomycin (47), forskolin (70), asiatic acid (71), and U-46619 (72). However, many MAPKKKs in the p38 module are shared by other MAPKs, especially the JNK module, and most of the treatments activate other MAPK isoforms in addition to p38 MAPKs (73) (Fig. S5). For example, anisomycin activates both p38 and JNK (47) (Fig. 6*A* and Fig. S6), whereas asiatic acid and U-46619 activate both p38 and ERK (71, 72). Thus, an agonist that selectively activates the p38 pathway is still lacking. MAPKs are involved in many cellular processes and can be activated by diverse upstream stimuli (45, 69, 74), so a compound(s) with specificity would be very helpful for better understanding of the individual pathways. The p38 MAPK–specific inhibitors SB203580 and SB202190 are widely used in research. Compounds LX-3, LX-4, and LX-5 could selectively activate the p38 MAPK pathway in multiple cell types (Fig. 6*A* and Fig. S6), which can serve as a useful tool to discriminate the p38 module from other MAPK modules; thus, they will hopefully have a role in future specific applications.

Finally, although we established a link between compounds LX-3, LX-4, and LX-5 and the p38 MAPK pathway, the exact targets of these compounds remain unknown. Clearly, future structure-activity relationship studies will help to optimize these compounds and potentially help to develop probes for target identification.

Experimental procedures

Cell culture and establishment of the reporter cell line

HEK293–derived cells and NIH 3T3 cells were cultured in DMEM (HyClone) supplemented with 10% FBS (Gibco) under standard conditions. MOLM13 cells were cultured in RPMI medium 1640 (Gibco) supplemented with 10% FBS (Gibco) under standard conditions. Transfections were performed with Lipofectamine 2000 (Invitrogen) according to the manufacturer's instructions.

Fig. S1*A* shows the procedures used to establish the reporter cell line. Briefly, the reporter vector pEGFP (or mCherry)-IRES-Puro-C1 was linearized by SphI (New England Biolabs) and then methylated *in vitro* by SssI methyltransferase (New England Biolabs). The methylated plasmids were co-transfected with pcDNA3.1-Hygro (+) (Invitrogen) at a ratio of 9:1 into HEK293 F cells. After hygromycin B (Amresco) selection, clones that exhibited an EGFP signal upon 5-aza-dC treatment, but not DMSO treatment, were further subcloned for selection. The selected subclones were also validated by analyzing their responses to 5-aza-dC and TSA and by DNA methylation status in the CMV promoter before and after 5-aza-dC treatment. The B2-17 clone, which exhibited low background and responded to 5-aza-dC with high sensitivity, was chosen for chemical screening.

High-content chemical screening

The compound library consisted of five sublibraries purchased from Maybridge, Enamine, Specs, Chemdiv, and WXTD. 5-aza-dC and TSA titrations were used as positive controls, and the same volume of DMSO was included as the negative control in each 384-well plate.

Before plating cells, 384-well plates (ViewPlate, PerkinElmer Life Sciences) were coated with poly-D-lysine (Sigma). For each well, 1,300 B2-17 cells were plated by using a Matrix Wellmate microplate dispenser (Thermo Scientific). Then 0.25 μl of compound was added to each well by using a versatile pipetting robot, the Biomek FX work station (Beckman Coulter), to give a final compound concentration of 5 μM. After treatment for 72 h, the cell nuclei were stained by Hoechst 33342 (Sigma) before imaging.

The cells were imaged with Opera LX (PerkinElmer Life Sciences; three views per well by using a $\times$10 (air) objective lens). Images were analyzed with the Columbus system, and the mean percentage of EGFP$^+$ cells (R_{GFP}) was obtained to extrapolate the number of EGFP-expressing cells and Hoechst-stained nuclei.

For the titration assay, the positive compounds were diluted in DMSO at concentrations ranging from 0.625 to 4 mM. Then

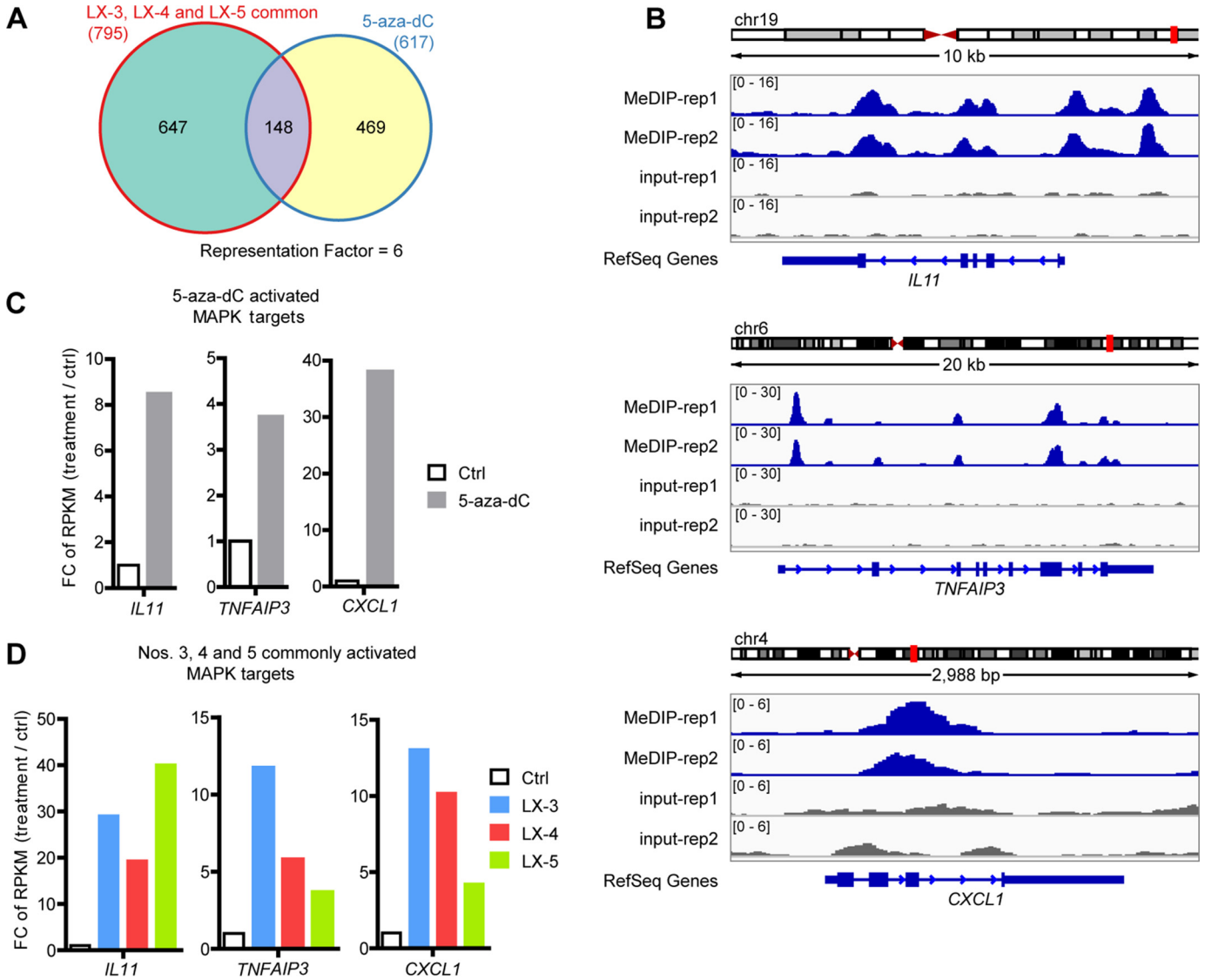

Figure 8. Compounds LX-3, LX-4, and LX-5 derepress a subset of endogenous methylated genes. *A*, Venn diagrams demonstrating the relationship between genes up-regulated by 5-aza-dC treatment and compound LX-3, LX-4, and LX-5 treatment. *B*, genome browser view of MeDIP-seq for three representative p38 MAPK pathway target genes (*IL11*, *TNFAIP3*, and *CXCL1*). The *scales* indicate read density from each sample normalized to 1 M sequencing depth. *C* and *D*, expression levels of the above p38 MAPK pathway target genes before and after treatment with 5-aza-dC (*C*) and compounds LX-3, LX-4, and LX-5 (*D*).

the B2-17 cells were treated by gradient compound and imaged as described before.

For each compound, a dose-response series was generated by using Origin Pro version 6.0 software. The dot plot was fit by a DoseResp curve, and then the EC_{50} was calculated.

Viability assays

HEK293 F cells were plated in 384-well, flat-bottom, tissue culture dishes (Corning Inc.) and treated with compounds, incubated 3 days, and assayed for viability using the CellTiter-Glo luminescent cell viability assay (Promega) according to the manufacturer's protocol. The absorbance at 490 and 650 nm (reference) was measured with an EnSight plate reader (PerkinElmer Life Sciences). Data were normalized to the untreated control (100% viability). Each treatment was tested in two independent assays, each containing three replicates. The titration-viability curves of each compound were also generated by using Origin Pro version 6.0 software.

RNAi

siRNAs were dissolved to 20 μM with diethyl pyrocarbonate (DEPC)-treated water. siRNA transfection was performed with Lipofectamine RNAiMax (Thermo, 13778150), and the final concentration of siRNA used was 10 nM. The knockdown efficiency was examined by qPCR, and the siRNA with the highest efficiency was selected to be used in this study.

UHPLC-MS/MS analysis

For sample preparation, 10 μg of genomic DNA was extracted using a genomic DNA purification kit (Promega). This DNA was incubated with a mixture of 1.0 unit of DNase I, 2.0 units of calf intestinal phosphatase, and 0.005 units of snake venom phosphodiesterase I at 37 °C for 24 h. The digest was filtered with ultrafiltration tubes and subjected to UHPLC-MS/MS analysis for detection of 5mC and 5hmC.

A UHPLC-MS/MS method has been developed for the detection of 5mC and 5hmC, as described previously for the measurement of 5mC and its oxidation products (75, 76). The Agilent 1290 Rapid Resolution LC system and a reverse-phase Zorbax SB-C18 2.1 × 100-mm column (1.8-μm particles) were applied in the UHPLC analysis. The digested DNA (5.0–10.0 μl) was injected onto the column, and nucleoside separation was accomplished by using a mobile phase of 95% water (containing 0.1% formic acid) and 5.0% methanol at a flow rate of 0.3 ml/min with isocratic elution. The stable isotope 5′-(methyl-d3) 2′-deoxycytidine was used as an internal standard for calibrating the quantitation of 5mC.

Bisulfite sequencing

Two micrograms of purified genomic DNA was bisulfite-converted using an EpiTect bisulfite kit (Qiagen) according to the manufacturer's instructions. DNA fragments of interest were PCR-amplified using Epi Taq (Takara), and purified PCR products were cloned into pMD18-T vectors (Takara). Positive clones were sequenced, and the results were analyzed using the BiQ analyzer (77). Primers for bisulfite sequencing were as follows: CMV-BS-F1, GGGTTATTAGTTTATAGTTTATATATGGA; CMV-BS-R1, ACCAAAATAAACACCACCCC.

RNA-seq and RT-qPCR

Total cell RNA was isolated using an RNeasy minikit (Qiagen), and cDNA was synthesized using a PrimeScript first-strand cDNA synthesis kit (Takara) with oligo(dT). Real-time qPCR was performed using 2× KAPA SYBR FAST qPCR Master Mix (Kapa Biosystems), and the results were normalized to the expression level of GAPDH. Primers for real-time PCR are listed in Table 1.

For high-throughput sequencing, total RNAs from two biological replicates were sent to BGI (Shenzhen, China) for RNA-seq library preparation and sequencing.

MeDIP-seq

MeDIP-seq was performed as described previously (78). Mouse monoclonal anti-5-methylcytidine antibody (BI-MECY-000) for MeDIP was purchased from Eurogentec.

Histone extraction and Western blotting

Histone proteins were extracted as described previously (79). Briefly, histones were acid-extracted from nuclei with 0.2 M H_2SO_4 for 2 h and precipitated with 33% TCA overnight. Samples were resuspended in 20–30 μl of double-distilled H_2O, and the protein concentration was calculated using the Bradford assay. Histones were separated by 15% SDS-PAGE and probed with anti-histone H4 acetylation (rabbit polyclonal, pan-acetyl, Millipore) and anti-histone H3 (rabbit polyclonal, 17168-1-AP, Proteintech) antibodies.

MAPK activation assays

HEK293 cells, MOLM13 cells, and NIH 3T3 cells were serum-starved for 8 h and then stimulated with EGF (100 ng/ml), anisomycin (30 μM) or compound LX-3 (5 μM), LX-4 (5 μM), or LX-5 (10 μM) for the indicated times. The activation of p44/42, JNK, and p38 was determined by Western blotting with antibodies specific for phosphorylated, activated forms of these kinases. We examined whether this activation occurred under our experimental conditions. Total lysates of cells were stimulated for different times, analyzed by SDS-PAGE, and immunoblotted with antibodies against activated p44/42, p38, and JNK. Total p44/42, p38, and JNK were monitored as loading controls.

Table 1
Primers used for real-time PCR

Gene	Primer
Human *GAPDH*	
Forward	GAAGGTGAAGGTCGGAGT
Reverse	GACAAGCTTCCCGTTCTCAG
Human *TNF*	
Forward	CACTTTGGAGTGATCGGCCC
Reverse	GAGGAGGTTGACCTTGGTCTG
Human *LY6K*	
Forward	TGCGAGACAACGAGATCCAG
Reverse	AACGCAGTATGGCTCTGTCC
Human *ISG20*	
Forward	TGCTGTGCTGTACGACAAGT
Reverse	GGAAGTCGTGCTTCAGGTCA
Human *EGR1*	
Forward	CCCGTTCGGATCCTTTCCTC
Reverse	GAGTGGTTTGGCTGGGGTAA
Human *IL11*	
Forward	CTCCCAGGTGTGCTGACAAG
Reverse	TAGGGGGAGATAATGGCGGG
Human *TNFAIP3*	
Forward	GGCTGCGTGTATTTTGGGAC
Reverse	CTGGCTCGATCTCAGTTGCT
Human *CXCL1*	
Forward	ACACTCAAGAATGGGCGGAA
Reverse	ACTTGGGGTTGACATTTCAAAAAGA
Mouse *Gapdh*	
Forward	CCCTTAAGAGGGATGCTGCC
Reverse	ACTGTGCCGTTGAATTTGCC
Mouse *Il11*	
Forward	CTTGATGTCCTACCTCCGGC
Reverse	GATCACAGGTTGGTCTGGGG
Mouse *Tnfaip3*	
Forward	AGGACTTTGCTACGACACTCG
Reverse	GCGAAGTTCAGGTCCACTGT
Mouse *Cxcl1*	
Forward	TGCACCCAAACCGAAGTCAT
Reverse	TTGTCAGAAGCCAGCGTTCA

Compounds and cytokines

5-aza-dC, TSA, sodium butyrate (NaB), RG108, and procaine were purchased from Sigma. The inhibitors SB203582, SP600125, trametinib, and FR180204 and the activator anisomycin were purchased from Selleck. The human EGF cytokine was purchased from Peprotech.

Antibodies

Mouse monoclonal anti-5-methylcytidine antibody (BI-MECY-000) for MeDIP was purchased from Eurogentec. Rabbit polyclonal anti-histone H4 acetylation antibody (pan-acetyl) was purchased from Millipore. Rabbit polyclonal anti-histone H3 antibody (17168-1-AP) was purchased from Proteintech. Mouse monoclonal anti-ERK antibody (sc-514302), anti-Phos-ERK (sc-7383), anti-JNK (sc-7345), anti-Phos-JNK (sc-6254), and anti-p38 antibodies (sc-7972) were purchased from Santa Cruz Biotechnology. Rabbit monoclonal anti-Phos-

p38 antibody (4511T) was purchased from Cell Signaling Technology.

Bioinformatics

For mRNA-seq, 50-bp single-end reads were generated by BGISEQ-500 platforms (BGI). Sequencing qualities were evaluated using FastQC software. Sequences were aligned with human genome hg19 using TopHat, and RPKM values were quantified using Cufflinks version 2.0.2. Up-regulated and down-regulated genes were defined by $|\log2(\text{treat/ctrl})| >= 1$, and both RPKM values were added to a pseudo-value of 0.5 to avoid being divided by zero.

GSEA analysis was performed using GSEA (80, 81) against three MAPK-related gene sets. For GO analysis, the identified hits were subjected to functional annotation clustering using the DAVID Bioinformatics Resources version 6.7 with default settings (82, 83). The tested categories are Biological Processes and KEGG. Enrichment results were grouped and visualized by the EnrichmentMap module in Cytoscape 3 (84). TFBS enrichment analysis was calculated by AME tools from the MEME suite (26) with default settings.

MeDIP-seq reads were generated by Illumina HiSeq-2000 platforms (single end, 50 bp). Sequencing qualities were evaluated using FASTQC software, and the reads were then aligned to hg19 genome sequences (<2 bp mismatches allowed). Only uniquely mapped reads were kept. Mapped reads were extended to the average fragment sizes. Genome profile files were generated with IGV tools and linearly normalized to the same depth of 10 million reads. TSS annotation data were obtained from the "refGene" table of UCSC hg19 databases. Read densities of MeDIP-seq for specific gene sets were averaged based on "bigwig" signals generated from reads mapping files.

Data availability

All high-throughput sequencing data have been deposited under GEO accession number GSE106573.

Author contributions—X. Li, E. S., Q. D., Y. L., J. Z., S. X., Z. Zhao, W. S., C. L., Y. Z., H. W., X. Lei, B. Z., and Z. Zhang resources; X. Li, E. S., Q. D., Y. L., J. Z., S. X., W. S., and C. L. data curation; X. Li, J. Z., and Z. Zhang software; X. Li, Q. D., and Z. Zhang formal analysis; X. Li, Q. D., S. X., and Z. Zhang validation; X. Li, B. Z., and Z. Zhang investigation; X. Li visualization; X. Li, E. S., Q. D., J. Z., S. X., H. W., X. Lei, B. Z., and Z. Zhang methodology; X. Li and Z. Zhang writing-original draft; X. Li, X. Lei, B. Z., and Z. Zhang project administration; E. S., Y. L., H. W., X. Lei, B. Z., and Z. Zhang writing-review and editing; X. Lei and B. Z. conceptualization; X. Lei and B. Z. supervision; B. Z. and Z. Zhang funding acquisition.

Acknowledgments—We thank the Chemistry Center and Imaging Facility at the National Institute of Biological Sciences, Beijing (NIBS), for helping with the high-throughput screening. We thank the Biological Resource Center at NIBS for synthesizing siRNAs. We thank Junying Jia and Shuang Sun from the FACS facility at the Institute of Biophysics, Chinese Academy of Sciences, for technical support.

References

1. Li, E., and Zhang, Y. (2014) DNA methylation in mammals. *Cold Spring Harb. Perspect. Biol.* **6,** a019133 CrossRef Medline
2. Allis, C. D., Jenuwein, T., and Reinberg, D., eds (2007) *Epigenetics*, pp. 341–355, Cold Spring Harbor Laboratory Press, Cold Spring Harbor, NY
3. Robertson, K. D. (2005) DNA methylation and human disease. *Nat. Rev. Genet.* **6,** 597–610 CrossRef Medline
4. Weber, M., Davies, J. J., Wittig, D., Oakeley, E. J., Haase, M., Lam, W. L., and Schübeler, D. (2005) Chromosome-wide and promoter-specific analyses identify sites of differential DNA methylation in normal and transformed human cells. *Nat. Genet.* **37,** 853–862 CrossRef Medline
5. Feinberg, A. P., and Tycko, B. (2004) The history of cancer epigenetics. *Nat. Rev. Cancer* **4,** 143–153 CrossRef Medline
6. Widschwendter, M., Jiang, G., Woods, C., Müller, H. M., Fiegl, H., Goebel, G., Marth, C., Müller-Holzner, E., Zeimet, A. G., Laird, P. W., and Ehrlich, M. (2004) DNA hypomethylation and ovarian cancer biology. *Cancer Res.* **64,** 4472–4480 CrossRef Medline
7. De Smet, C., Lurquin, C., Lethé, B., Martelange, V., and Boon, T. (1999) DNA methylation is the primary silencing mechanism for a set of germ line- and tumor-specific genes with a CpG-rich promoter. *Mol. Cell. Biol.* **19,** 7327–7335 CrossRef Medline
8. Laird, P. W. (2003) The power and the promise of DNA methylation markers. *Nat. Rev. Cancer* **3,** 253–266 CrossRef Medline
9. Verkerk, A. J., Pieretti, M., Sutcliffe, J. S., Fu, Y.-H., Kuhl, D. P., Pizzuti, A., Reiner, O., Richards, S., Victoria, M. F., and Zhang, F. P. (1991) Identification of a gene (FMR-1) containing a CGG repeat coincident with a breakpoint cluster region exhibiting length variation in fragile X syndrome. *Cell* **65,** 905–914 CrossRef Medline
10. Campuzano, V., Montermini, L., Moltò, M. D., Pianese, L., Cossée, M., Cavalcanti, F., Monros, E., Rodius, F., Duclos, F., Monticelli, A., Zara, F., Cañizares, J., Koutnikova, H., Bidichandani, S. I., Gellera, C., *et al.* (1996) Friedreich's ataxia: autosomal recessive disease caused by an intronic GAA triplet repeat expansion. *Science* **271,** 1423–1427 CrossRef Medline
11. Lefebvre, S., Bürglen, L., Reboullet, S., Clermont, O., Burlet, P., Viollet, L., Benichou, B., Cruaud, C., Millasseau, P., and Zeviani, M. (1995) Identification and characterization of a spinal muscular atrophy-determining gene. *Cell* **80,** 155–165 CrossRef Medline
12. Boyes, J., and Bird, A. (1991) DNA methylation inhibits transcription indirectly via a methyl-CpG binding protein. *Cell* **64,** 1123–1134 CrossRef Medline
13. Meehan, R. R., Lewis, J. D., and Bird, A. P. (1992) Characterization of MeCP2, a vertebrate DNA binding protein with affinity for methylated DNA. *Nucleic Acids Res.* **20,** 5085–5092 CrossRef Medline
14. Eden, S., Hashimshony, T., Keshet, I., Cedar, H., and Thorne, A. (1998) DNA methylation models histone acetylation. *Nature* **394,** 842–842 CrossRef Medline
15. Jones, P. L., Veenstra, G. C. J., Wade, P. A., Vermaak, D., Kass, S. U., Landsberger, N., Strouboulis, J., and Wolffe, A. P. (1998) Methylated DNA and MeCP2 recruit histone deacetylase to repress transcription. *Nat. Genet.* **19,** 187–191 CrossRef Medline
16. Nan, X., Ng, H.-H., Johnson, C. A., Laherty, C. D., Turner, B. M., Eisenman, R. N., and Bird, A. (1998) Transcriptional repression by the methyl-CpG-binding protein MeCP2 involves a histone deacetylase complex. *Nature* **393,** 386–389 CrossRef Medline
17. Zhang, Y., Ng, H.-H., Erdjument-Bromage, H., Tempst, P., Bird, A., and Reinberg, D. (1999) Analysis of the NuRD subunits reveals a histone deacetylase core complex and a connection with DNA methylation. *Genes Dev.* **13,** 1924–1935 CrossRef Medline
18. Stresemann, C., Brueckner, B., Musch, T., Stopper, H., and Lyko, F. (2006) Functional diversity of DNA methyltransferase inhibitors in human cancer cell lines. *Cancer Res.* **66,** 2794–2800 CrossRef Medline
19. Cameron, E. E., Bachman, K. E., Myöhänen, S., Herman, J. G., and Baylin, S. B. (1999) Synergy of demethylation and histone deacetylase inhibition in the re-expression of genes silenced in cancer. *Nat. Genet.* **21,** 103–107 CrossRef Medline

20. Herman, D., Jenssen, K., Burnett, R., Soragni, E., Perlman, S. L., and Gottesfeld, J. M. (2006) Histone deacetylase inhibitors reverse gene silencing in Friedreich's ataxia. *Nat. Chem. Biol.* **2,** 551–558 CrossRef Medline
21. Suzuki, H., Gabrielson, E., Chen, W., Anbazhagan, R., van Engeland, M., Weijenberg, M. P., Herman, J. G., and Baylin, S. B. (2002) A genomic screen for genes upregulated by demethylation and histone deacetylase inhibition in human colorectal cancer. *Nat. Genet.* **31,** 141–149 CrossRef Medline
22. Daskalakis, M., Nguyen, T. T., Nguyen, C., Guldberg, P., Köhler, G., Wijermans, P., Jones, P. A., and Lübbert, M. (2002) Demethylation of a hypermethylated P15/INK4B gene in patients with myelodysplastic syndrome by 5-Aza-2′-deoxycytidine (decitabine) treatment. *Blood* **100,** 2957–2964 CrossRef Medline
23. Yamashita, S., Tsujino, Y., Moriguchi, K., Tatematsu, M., and Ushijima, T. (2006) Chemical genomic screening for methylation-silenced genes in gastric cancer cell lines using 5-aza-2′-deoxycytidine treatment and oligonucleotide microarray. *Cancer Sci.* **97,** 64–71 CrossRef Medline
24. Coffee, B., Zhang, F., Warren, S. T., and Reines, D. (1999) Acetylated histones are associated with FMR1 in normal but not fragile X-syndrome cells. *Nat. Genet.* **22,** 98–101 CrossRef Medline
25. Lynch, C. A., Tycko, B., Bestor, T. H., and Walsh, C. P. (2002) Reactivation of a silenced H19 gene in human rhabdomyosarcoma by demethylation of DNA but not by histone hyperacetylation. *Mol. Cancer* **1,** 2 CrossRef Medline
26. McLeay, R. C., and Bailey, T. L. (2010) Motif enrichment analysis: a unified framework and an evaluation on ChIP data. *BMC Bioinformatics* **11,** 165 CrossRef Medline
27. Steele, N., Finn, P., Brown, R., and Plumb, J. (2009) Combined inhibition of DNA methylation and histone acetylation enhances gene re-expression and drug sensitivity *in vivo*. *Br. J. Cancer* **100,** 758–763 CrossRef Medline
28. Benjamin, D., and Jost, J.-P. (2001) Reversal of methylation-mediated repression with short-chain fatty acids: evidence for an additional mechanism to histone deacetylation. *Nucleic Acids Res.* **29,** 3603–3610 CrossRef Medline
29. Tate, P. H., and Bird, A. P. (1993) Effects of DNA methylation on DNA-binding proteins and gene expression. *Curr. Opin. Genet. Dev.* **3,** 226–231 CrossRef Medline
30. Watt, F., and Molloy, P. L. (1988) Cytosine methylation prevents binding to DNA of a HeLa cell transcription factor required for optimal expression of the adenovirus major late promoter. *Genes Dev.* **2,** 1136–1143 CrossRef Medline
31. Prendergast, G. C., Lawe, D., and Ziff, E. B. (1991) Association of Myn, the murine homolog of max, with c-Myc stimulates methylation-sensitive DNA binding and ras cotransformation. *Cell* **65,** 395–407 CrossRef Medline
32. Sun, L., Wang, H., Wang, Z., He, S., Chen, S., Liao, D., Wang, L., Yan, J., Liu, W., Lei, X., and Wang, X. (2012) Mixed lineage kinase domain-like protein mediates necrosis signaling downstream of RIP3 kinase. *Cell* **148,** 213–227 CrossRef Medline
33. Wang, G., Wang, X., Yu, H., Wei, S., Williams, N., Holmes, D. L., Halfmann, R., Naidoo, J., Wang, L., Li, L., Chen, S., Harran, P., Lei, X., and Wang, X. (2013) Small-molecule activation of the TRAIL receptor DR5 in human cancer cells. *Nat. Chem. Biol.* **9,** 84–89 CrossRef Medline
34. Dong, T., Li, C., Wang, X., Dian, L., Zhang, X., Li, L., Chen, S., Cao, R., Li, L., Huang, N., He, S., and Lei, X. (2015) Ainsliadimer A selectively inhibits IKKα/β by covalently binding a conserved cysteine. *Nat. Commun.* **6,** 6522 CrossRef Medline
35. Li, D., Li, C., Li, L., Chen, S., Wang, L., Li, Q., Wang, X., Lei, X., and Shen, Z. (2016) Natural product kongensin A is a non-canonical HSP90 inhibitor that blocks RIP3-dependent necroptosis. *Cell Chem. Biol.* **23,** 257–266 CrossRef Medline
36. Pieper, H. C., Evert, B. O., Kaut, O., Riederer, P. F., Waha, A., and Wüllner, U. (2008) Different methylation of the TNF-α promoter in cortex and substantia nigra: implications for selective neuronal vulnerability. *Neurobiol. Dis.* **32,** 521–527 CrossRef Medline
37. Campión, J., Milagro, F. I., Goyenechea, E., and Martínez, J. A. (2009) TNF-α promoter methylation as a predictive biomarker for weight-loss response. *Obesity* **17,** 1293–1297 Medline
38. Kong, H. K., Yoon, S., and Park, J. H. (2012) The regulatory mechanism of the LY6K gene expression in human breast cancer cells. *J. Biol. Chem.* **287,** 38889–38900 CrossRef Medline
39. Brueckner, B., Garcia Boy, R., Siedlecki, P., Musch, T., Kliem, H. C., Zielenkiewicz, P., Suhai, S., Wiessler, M., and Lyko, F. (2005) Epigenetic reactivation of tumor suppressor genes by a novel small-molecule inhibitor of human DNA methyltransferases. *Cancer Res.* **65,** 6305–6311 CrossRef Medline
40. Ono, K., and Han, J. (2000) The p38 signal transduction pathway activation and function. *Cell. Signal.* **12,** 1–13 CrossRef Medline
41. Phong, M. S., Van Horn, R. D., Li, S., Tucker-Kellogg, G., Surana, U., and Ye, X. S. (2010) p38 mitogen-activated protein kinase promotes cell survival in response to DNA damage but is not required for the G2 DNA damage checkpoint in human cancer cells. *Mol. Cell. Biol.* **30,** 3816–3826 CrossRef Medline
42. Gazel, A., Banno, T., Walsh, R., and Blumenberg, M. (2006) Inhibition of JNK promotes differentiation of epidermal keratinocytes. *J. Biol. Chem.* **281,** 20530–20541 CrossRef Medline
43. Pearson, G., Robinson, F., Beers Gibson, T., Xu, B.-E., Karandikar, M., Berman, K., and Cobb, M. H. (2001) Mitogen-activated protein (MAP) kinase pathways: regulation and physiological functions. *Endocr. Rev.* **22,** 153–183 CrossRef Medline
44. Su, B., and Karin, M. (1996) Mitogen-activated protein kinase cascades and regulation of gene expression. *Curr. Opin. Immunol.* **8,** 402–411 CrossRef Medline
45. Cargnello, M., and Roux, P. P. (2011) Activation and function of the MAPKs and their substrates, the MAPK-activated protein kinases. *Microbiol. Mol. Biol. Rev.* **75,** 50–83 CrossRef Medline
46. Szklarczyk, D., Morris, J. H., Cook, H., Kuhn, M., Wyder, S., Simonovic, M., Santos, A., Doncheva, N. T., Roth, A., and Bork, P., Jensen, L. J., and von Mering, C. (2017) The STRING database in 2017: quality-controlled protein–protein association networks, made broadly accessible. *Nucleic Acids Res.* **45,** D362–D368 CrossRef Medline
47. Cano, E., Hazzalin, C. A., and Mahadevan, L. C. (1994) Anisomycin-activated protein kinases p45 and p55 but not mitogen-activated protein kinases ERK-1 and-2 are implicated in the induction of c-fos and c-jun. *Mol. Cell. Biol.* **14,** 7352–7362 CrossRef Medline
48. Zhang, C., Baumgartner, R. A., Yamada, K., and Beaven, M. A. (1997) Mitogen-activated Protein (MAP) kinase regulates production of tumor necrosis factor-α and release of arachidonic acid in mast cells indications of communication between p38 and p42 Map kinases. *J. Biol. Chem.* **272,** 13397–13402 CrossRef Medline
49. Gould, G. W., Cuenda, A., Thomson, F. J., and Cohen, P. (1995) The activation of distinct mitogen-activated protein kinase cascades is required for the stimulation of 2-deoxyglucose uptake by interleukin-1 and insulin-like growth factor-1 in KB cells. *Biochem. J.* **311,** 735–738 CrossRef Medline
50. Cano, E., Doza, Y. N., Ben-Levy, R., Cohen, P., and Mahadevan, L. C. (1996) Identification of anisomycin-activated kinases p45 and p55 in murine cells. *Oncogene* **12,** 805–812 Medline
51. Minden, A., Lin, A., McMahon, M., Lange-Carter, C., Dérijard, B., Davis, R. J., Johnson, G. L., and Karin, M. (1994) Differential activation of ERK and JNK mitogen-activated protein kinases by Raf-1 and MEKK. *Science* **266,** 1719–1723 CrossRef Medline
52. Ohori, M., Kinoshita, T., Okubo, M., Sato, K., Yamazaki, A., Arakawa, H., Nishimura, S., Inamura, N., Nakajima, H., Neya, M., Miyake, H., and Fujii, T. (2005) Identification of a selective ERK inhibitor and structural determination of the inhibitor–ERK2 complex. *Biochem. Biophys. Res. Commun.* **336,** 357–363 CrossRef Medline
53. Young, P. R., McLaughlin, M. M., Kumar, S., Kassis, S., Doyle, M. L., McNulty, D., Gallagher, T. F., Fisher, S., McDonnell, P. C., Carr, S. A., Huddleston, M. J., Seibel, G., Porter, T. G., Livi, G. P., Adams, J. L., and Lee, J. C. (1997) Pyridinyl imidazole inhibitors of p38 mitogen-activated protein kinase bind in the ATP site. *J. Biol. Chem.* **272,** 12116–12121 CrossRef Medline
54. Bennett, B. L., Sasaki, D. T., Murray, B. W., O'Leary, E. C., Sakata, S. T., Xu, W., Leisten, J. C., Motiwala, A., Pierce, S., Satoh, Y., Bhagwat, S. S., Manning, A. M., and Anderson, D. W. (2001) SP600125, an anthrapyrazolone

inhibitor of Jun N-terminal kinase. *Proc. Natl. Acad. Sci. U.S.A.* **98,** 13681–13686 CrossRef Medline
55. Raingeaud, J., Whitmarsh, A. J., Barrett, T., Dérijard, B., and Davis, R. J. (1996) MKK3- and MKK6-regulated gene expression is mediated by the p38 mitogen-activated protein kinase signal transduction pathway. *Mol. Cell. Biol.* **16,** 1247–1255 CrossRef Medline
56. Zer, C., Sachs, G., and Shin, J. M. (2007) Identification of genomic targets downstream of p38 mitogen-activated protein kinase pathway mediating tumor necrosis factor-α signaling. *Physiol. Genomics* **31,** 343–351 CrossRef Medline
57. Cheng, J. C., Matsen, C. B., Gonzales, F. A., Ye, W., Greer, S., Marquez, V. E., Jones, P. A., and Selker, E. U. (2003) Inhibition of DNA methylation and reactivation of silenced genes by zebularine. *J. Natl. Cancer Inst.* **95,** 399–409 CrossRef Medline
58. Santi, D. V., Norment, A., and Garrett, C. E. (1984) Covalent bond formation between a DNA-cytosine methyltransferase and DNA containing 5-azacytosine. *Proc. Natl. Acad. Sci. U.S.A.* **81,** 6993–6997 CrossRef Medline
59. Fernandez, J. M., and Hoeffler, J. P. (1998) *Gene Expression Systems: Using Nature for the Art of Expression*, pp. 211–218, Academic Press, Inc., New York
60. Iguchi-Ariga, S., and Schaffner, W. (1989) CpG methylation of the cAMP-responsive enhancer/promoter sequence TGACGTCA abolishes specific factor binding as well as transcriptional activation. *Genes Dev.* **3,** 612–619
61. Tierney, R. J., Kirby, H. E., Nagra, J. K., Desmond, J., Bell, A. I., and Rickinson, A. B. (2000) Methylation of transcription factor binding sites in the Epstein-Barr virus latent cycle promoter Wp coincides with promoter down-regulation during virus-induced B-cell transformation. *J. Virol.* **74,** 10468–10479 CrossRef Medline
62. Xing, J., Ginty, D. D., and Greenberg, M. E. (1996) Coupling of the RAS-MAPK pathway to gene activation by RSK2, a growth factor-regulated CREB kinase. *Science* **273,** 959–963 CrossRef Medline
63. Deak, M., Clifton, A. D., Lucocq, L. M., and Alessi, D. R. (1998) Mitogen- and stress-activated protein kinase-1 (MSK1) is directly activated by MAPK and SAPK2/p38, and may mediate activation of CREB. *EMBO J.* **17,** 4426–4441 CrossRef Medline
64. Tan, Y., Rouse, J., Zhang, A., Cariati, S., Cohen, P., and Comb, M. (1996) FGF and stress regulate CREB and ATF-1 via a pathway involving p38 MAP kinase and MAPKAP kinase-2. *EMBO J.* **15,** 4629–4642 Medline
65. Montminy, M. R., Sevarino, K. A., Wagner, J. A., Mandel, G., and Goodman, R. H. (1986) Identification of a cyclic-AMP-responsive element within the rat somatostatin gene. *Proc. Natl. Acad. Sci. U.S.A.* **83,** 6682–6686 CrossRef Medline
66. Short, J. M., Wynshaw-Boris, A., Short, H. P., and Hanson, R. (1986) Characterization of the phosphoenolpyruvate carboxykinase (GTP) promoter-regulatory region. II. Identification of cAMP and glucocorticoid regulatory domains. *J. Biol. Chem.* **261,** 9721–9726 Medline
67. Comb, M., Birnberg, N. C., Seasholtz, A., Herbert, E., and Goodman, H. M. (1986) A cyclic AMP-and phorbol ester-inducible DNA element. *Nature* **323,** 353–356 CrossRef Medline
68. Chang, L., and Karin, M. (2001) Mammalian MAP kinase signalling cascades. *Nature* **410,** 37–40 CrossRef Medline
69. Zarubin, T., and Han, J. (2005) Activation and signaling of the p38 MAP kinase pathway. *Cell Res.* **15,** 11–18 CrossRef Medline
70. Hansen, T. O., Rehfeld, J. F., and Nielsen, F. C. (2000) Cyclic AMP-induced neuronal differentiation via activation of p38 mitogen-activated protein kinase. *J. Neurochem.* **75,** 1870–1877 Medline
71. Hsu, Y.-L., Kuo, P.-L., Lin, L.-T., and Lin, C.-C. (2005) Asiatic acid, a triterpene, induces apoptosis and cell cycle arrest through activation of extracellular signal-regulated kinase and p38 mitogen-activated protein kinase pathways in human breast cancer cells. *J. Pharmacol. Exp. Ther.* **313,** 333–344 Medline
72. Saklatvala, J., Rawlinson, L., Waller, R. J., Sarsfield, S., Lee, J. C., Morton, L. F., Barnes, M. J., and Farndale, R. W. (1996) Role for p38 mitogen-activated protein kinase in platelet aggregation caused by collagen or a thromboxane analogue. *J. Biol. Chem.* **271,** 6586–6589 CrossRef Medline
73. Cuadrado, A., and Nebreda, A. R. (2010) Mechanisms and functions of p38 MAPK signalling. *Biochem. J.* **429,** 403–417 CrossRef Medline
74. Johnson, G. L., and Lapadat, R. (2002) Mitogen-activated protein kinase pathways mediated by ERK, JNK, and p38 protein kinases. *Science* **298,** 1911–1912 CrossRef Medline
75. Yin, R., Mao, S.-Q., Zhao, B., Chong, Z., Yang, Y., Zhao, C., Zhang, D., Huang, H., Gao, J., Li, Z., Jiao, Y., Li, C., Liu, S., Wu, D. Gu, W., *et al.* (2013) Ascorbic acid enhances Tet-mediated 5-methylcytosine oxidation and promotes DNA demethylation in mammals. *J. Am. Chem. Soc.* **135,** 10396–10403 CrossRef Medline
76. Zhao, B., Yang, Y., Wang, X., Chong, Z., Yin, R., Song, S.-H., Zhao, C., Li, C., Huang, H., and Sun, B.-F. (2013) Redox-active quinones induces genome-wide DNA methylation changes by an iron-mediated and Tet-dependent mechanism. *Nucleic Acids Res.* **42,** 1593–1605
77. Bock, C., Reither, S., Mikeska, T., Paulsen, M., Walter, J., and Lengauer, T. (2005) BiQ Analyzer: visualization and quality control for DNA methylation data from bisulfite sequencing. *Bioinformatics* **21,** 4067–4068 CrossRef Medline
78. Xiong, J., Zhang, Z., Chen, J., Huang, H., Xu, Y., Ding, X., Zheng, Y., Nishinakamura, R., Xu, G.-L., Wang, H., Chen, S., Gao, S., and Zhu, B. (2016) Cooperative action between SALL4A and TET proteins in stepwise oxidation of 5-methylcytosine. *Mol. Cell* **64,** 913–925 CrossRef Medline
79. Shechter, D., Dormann, H. L., Allis, C. D., and Hake, S. B. (2007) Extraction, purification and analysis of histones. *Nat. Protoc.* **2,** 1445–1457 CrossRef Medline
80. Subramanian, A., Tamayo, P., Mootha, V. K., Mukherjee, S., Ebert, B. L., Gillette, M. A., Paulovich, A., Pomeroy, S. L., Golub, T. R., Lander, E. S., and Mesirov, J. P. (2005) Gene set enrichment analysis: a knowledge-based approach for interpreting genome-wide expression profiles. *Proc. Natl. Acad. Sci. U.S.A.* **102,** 15545–15550 CrossRef Medline
81. Mootha, V. K., Lindgren, C. M., Eriksson, K. F., Subramanian, A., Sihag, S., Lehar, J., Puigserver, P., Carlsson, E., Ridderstråle, M., Laurila, E., Houstis, N., Daly, M. J., Patterson, N., Mesirov, J. P., Golub, T. R., *et al.* (2003) PGC-1 α-responsive genes involved in oxidative phosphorylation are coordinately downregulated in human diabetes. *Nat. Genet.* **34,** 267–273 CrossRef Medline
82. Huang, D. W., Sherman, B. T., and Lempicki, R. A. (2009) Systematic and integrative analysis of large gene lists using DAVID bioinformatics resources. *Nat. Protoc.* **4,** 44–57 CrossRef Medline
83. Huang, D. W., Sherman, B. T., and Lempicki, R. A. (2009) Bioinformatics enrichment tools: paths toward the comprehensive functional analysis of large gene lists. *Nucleic Acids Res.* **37,** 1–13 CrossRef Medline
84. Shannon, P., Markiel, A., Ozier, O., Baliga, N. S., Wang, J. T., Ramage, D., Amin, N., Schwikowski, B., and Ideker, T. (2003) Cytoscape: a software environment for integrated models of biomolecular interaction networks. *Genome Res.* **13,** 2498–2504 CrossRef Medline